LONG-DISTANCE SOUND PROPAGATION OVER DISCONTINUOUS IMPEDANCES

Simon N. Chandler-Wilde, Joseph N. B. Harriott
and David C. Hothersall
Department of Civil Engineering, Bradford University, England.

SUMMARY

A calculation method is presented for sound propagation over an impedance discontinuity in flat ground with a homogeneous, still atmosphere. The method is based on an approximate solution to a two dimensional boundary integral equation formulation of the problem, which expresses the wave field as the solution for homogeneous ground plus an integral over half of the boundary. Through recognising this integral as a generalised Fourier integral, asymptotic methods are applied to evaluate the part of the integral most expensive to compute by numerical quadrature. Single frequency excess attenuation results for propagation from a point source above rigid ground to a receiver above absorbing ground are discussed. The results are applied, with air attenuation and A-weighting, to a notional jet engine noise source; simple trends are noted.

INTRODUCTION

The problem discussed in this paper is propagation from a point source in a homogeneous still atmosphere above flat locally reacting ground. Efficient calculation methods for the wave field above acoustically homogeneous ground are well known (e.g. ref. 1). More recently sound propagation over impedance inhomogeneities has been theoretically examined; a thorough review is given in reference 2. A limitation of the accurate calculation methods is their computational expense.

Here we focus on propagation over a single straight line impedance discontinuity which lies perpendicular to the direct source-receiver propagation path. A development to an existing calculation method is described which significantly reduces the computational expense.

The improved calculation method is applied to grazing incidence propagation from a source above a rigid surface to a distant receiver above absorbing ground. Monofrequency excess attenuation results are examined and some simple trends are observed. The results for a 1·5m high receiver are applied, with air attenuation and A-weighting, to a notional jet engine noise source at 1·5m height. Again some simple trends are noted.

CALCULATION METHOD

Description of the Problem

Figure 1 illustrates the problem. A point source with harmonic time dependence ($e^{-i\omega t}$) is situated over a flat locally reacting surface of infinite extent. The surface is divided by a straight line into two half planes. Each half plane is acoustically homogeneous and characterised by a frequency dependent complex admittance (the inverse of the normalised acoustic surface impedance). We are interested in evaluating the acoustic potential at a point in a vertical half plane that is bounded by the surface, passes through the source and is perpendicular to the line of the admittance discontinuity. For the mathematical description we will use right-handed Cartesian coordinates Oxyz as indicated in Figure 1, the y-axis vertical and the surface in the plane y=0. The source and receiver coordinates are $(0,h_S,0)$ and $(L,h_r,0)$ respectively. The admittance discontinuity is along the line x=X in the surface.

An Existing Calculation Method

First we consider the related problem in which the source is replaced by an infinitely long coherent line source, parallel to the admittance discontinuity. This cylindrical wave propagation problem is mathematically equivalent to the two dimensional problem which is illustrated in Figure 2. From the mathematical expression of this problem as a two dimensional boundary value problem (consisting of the Helmholtz equation and suitable boundary conditions) the following boundary integral equation can be derived (ref. 3):

$$\Phi(\underset{\sim}{t}_2,\underset{\sim}{t}_1) = G_{\beta_2}(\underset{\sim}{t}_1,\underset{\sim}{t}_2) + ik(\beta_1-\beta_2)\int_{-\infty}^{X}\Phi(\underset{\sim}{s},\underset{\sim}{t}_1)G_{\beta_2}(\underset{\sim}{s},\underset{\sim}{t}_2)dx. \qquad (1)$$

In this equation $\underset{\sim}{t}_1=(0,h_S)$ is the source position, $\underset{\sim}{t}_2=(L,h_r)$ is the receiver position, and β_1 and β_2 are the admittances of the two halves of the boundary. The integration is over the interval $\gamma=(-\infty,X]$; this is the part of the boundary with admittance β_1. $\underset{\sim}{s}=(x,0)$ is a point in the boundary. For two points $\underset{\sim}{a}$ and $\underset{\sim}{b}$, $\Phi(\underset{\sim}{a},\underset{\sim}{b})$ denotes the acoustic potential detected by a receiver at $\underset{\sim}{a}$ when insonified by a unit source at $\underset{\sim}{b}$; $G_\beta(\underset{\sim}{a},\underset{\sim}{b})$ (where $\beta=\beta_1$ or β_2) denotes the same quantity in the simple case when the boundary has homogeneous admittance β. Efficient methods for evaluating the solution in this simpler case have already been developed (refs. 4,5).

Equation (1), which describes an inhomogeneous admittance boundary problem, can be solved accurately for $\Phi(\underset{\sim}{t}_2,\underset{\sim}{t}_1)$ by the boundary element method (refs. 3,4,6). We consider here an approximate but less computationally expensive method of solution. To develop this we make the physically plausible assumption that the potential in γ is what it would be if the whole boundary had admittance β_1 (refs. 7,8). Thus $\Phi(\underset{\sim}{s},\underset{\sim}{t}_1)$ in equation (1) is replaced by $G_{\beta_1}(\underset{\sim}{s},\underset{\sim}{t}_1)$, giving the following approximation to $\Phi(\underset{\sim}{t}_2,\underset{\sim}{t}_1)$:

$$\Phi_A(\underset{\sim}{t}_2,\underset{\sim}{t}_1) = G_{\beta_2}(\underset{\sim}{t}_1,\underset{\sim}{t}_2) + i(\beta_1-\beta_2)I(X) \ ,$$

where

$$I(X)= k\int_{-\infty}^{X} G_{\beta_1}(\underset{\sim}{s},\underset{\sim}{t}_1)G_{\beta_2}(\underset{\sim}{s},\underset{\sim}{t}_2)dx \ . \qquad (2)$$

This approximation avoids using the boundary element method.

Using $\Phi_A(\underset{\sim}{t}_2,\underset{\sim}{t}_1)$ we can calculate $Q_A(\underset{\sim}{t}_2,\underset{\sim}{t}_1)$, an approximate cylindrical wave reflection coefficient. Let d and D denote the distances from source and from image source (at $(0,-h_s)$) to receiver, respectively. Assuming a source with unit volume flow rate amplitude,

$$\Phi_A(\underset{\sim}{t}_2,\underset{\sim}{t}_1) = -\frac{i}{4}H_0^{(1)}(kd) + Q_A(\underset{\sim}{t}_2,\underset{\sim}{t}_1)\left[-\frac{i}{4}H_0^{(1)}(kD)\right] \quad ,$$

where $H_0^{(1)}$ is the Hankel function of the first kind of order zero.

For propagation over short distances, the difference $20\log_{10}|\Phi_A(\underset{\sim}{t}_2,\underset{\sim}{t}_1)| - 20\log_{10}|\Phi(\underset{\sim}{t}_2,\underset{\sim}{t}_1)|$, where $\Phi(\underset{\sim}{t}_2,\underset{\sim}{t}_1)$ is calculated by the boundary element method, has been found to be around 0·1dB (ref. 6). This suggests that $Q_A(\underset{\sim}{t}_2,\underset{\sim}{t}_1)$ is an accurate approximation to $Q(\underset{\sim}{t}_2,\underset{\sim}{t}_1)$, the exact cylindrical wave reflection coefficient for the two dimensional problem illustrated in Figure 2. Also, it has been argued that (ref. 6), for a receiver in the far field of the image source ($kD \gg 1$), $Q(\underset{\sim}{t}_2,\underset{\sim}{t}_1)$ is an accurate approximation to the spherical wave reflection coefficent, q, for the three dimensional problem illustrated in Figure 1. If the point source in the three dimensional problem has unit volume flow rate amplitude, then the acoustic potential at the receiver position is

$$\varphi = -\frac{e^{ikd}}{4\pi d} - q\frac{e^{ikD}}{4\pi D} \quad .$$

Replacing q with $Q(\underset{\sim}{t}_2,\underset{\sim}{t}_1)$, which is approximated by $Q_A(\underset{\sim}{t}_2,\underset{\sim}{t}_1)$, we obtain an approximation for φ:

$$\varphi_A = -\frac{e^{ikd}}{4\pi d} - Q_A(\underset{\sim}{t}_2,\underset{\sim}{t}_1)\frac{e^{ikD}}{4\pi D} \quad . \qquad (3)$$

We assume throughout the rest of the paper, without further comment, that this is a good approximation for φ.

The main computational expense in this approximate calculation method is in evaluating the integral I(X). In previous calculations (ref. 6) I(X) was evaluated numerically after first replacing the lower limit of integration, $-\infty$, by a sufficiently large negative value. Unfortunately the integrand in equation (2) is usually highly oscillatory over the range of integration, making numerical integration an expensive process. Here we derive a semi-analytical method of evaluation which deals efficiently with the part of the integral that is most expensive to evaluate numerically.

The Improved Calculation Method

We begin by examining the general behaviour of the integrand in equation (2). We note that, for a receiver at the point $\underset{\sim}{s}$ in the boundary, we can write

$$4iG_\beta(\underset{\sim}{s},\underset{\sim}{t}) = H_0^{(1)}(k|\underset{\sim}{t}-\underset{\sim}{s}|)R_\beta(\underset{\sim}{s},\underset{\sim}{t}) \quad ,$$

where $R_\beta(\underset{\sim}{s},\underset{\sim}{t})=1+Q_\beta(\underset{\sim}{s},\underset{\sim}{t})$, and $Q_\beta(\underset{\sim}{s},\underset{\sim}{t})$ is the cylindrical wave reflection coefficient for a homogeneous surface of admittance β. As x is increased from $-\infty$, the real and imaginary parts of $H_0^{(1)}(k|\underset{\sim}{t}-\underset{\sim}{s}|)$ oscillate in a well defined fashion, while $R_\beta(\underset{\sim}{s},\underset{\sim}{t})$ changes less rapidly. In fact, from the asymptotic expansion of the Hankel function at large argument, we see that if we factorise,

$$G_\beta(\underset{\sim}{s},\underset{\sim}{t}) = e^{ik|\underset{\sim}{t}-\underset{\sim}{s}|}S(\underset{\sim}{s},\underset{\sim}{t}) \quad ,$$

then $S(\underset{\sim}{s},\underset{\sim}{t})$ is smooth as a function of x compared to $e^{ik|\underset{\sim}{t}-\underset{\sim}{s}|}$ when $k|\underset{\sim}{t}-\underset{\sim}{s}|$ is large. This observation suggests that I(X) can be usefully written in the form of a generalised Fourier integral:

$$I(X) = \int_{-\infty}^{X} f(x) e^{ikg(x)} dx \quad , \tag{4}$$

where

$$f(x) = kG_{\beta_1}(\underset{\sim}{s},\underset{\sim}{t}_1)G_{\beta_2}(\underset{\sim}{s},\underset{\sim}{t}_2)e^{-ikg(x)},$$

$$g(x) = g_1(x) + g_2(x),$$

and

$$g_1(x) = |\underset{\sim}{t}_1-\underset{\sim}{s}|, \quad g_2(x) = |\underset{\sim}{t}_2-\underset{\sim}{s}|.$$

Notice that g(x) is the distance from source to receiver via the point $\underset{\sim}{s}$. The location on the boundary of the geometrical reflection point, x_r, is therefore given by $g'(x_r)=0$. When $\underset{\sim}{s}$ is sufficiently distant from $\underset{\sim}{t}_1$, $\underset{\sim}{t}_2$, and $(x_r,0)$, f(x) is a slowly changing function of x compared to $e^{ikg(x)}$. This fact allows us to use simple asymptotic methods to help evaluate I(X).

To introduce the asymptotic analysis we consider first what proves to be the simplest type of configuration to deal with. This has x_r well outside γ, and $\underset{\sim}{t}_1$ and $\underset{\sim}{t}_2$ at least one wavelength from the boundary. For this type of configuration we may integrate I(X) by parts to give

$$I(X) = J_1(X) + R_1(X) \tag{5}$$

where

$$J_1(X) = \frac{f(X)\, e^{ikg(X)}}{ikg'(X)} \quad ,$$

$$R_1(X) = -\int_{-\infty}^{X} \frac{d}{dx}\left[\frac{f(x)}{ikg'(x)}\right] e^{ikg(x)} dx \quad ,$$

and then integrate $R_1(X)$ by parts to give

$$R_1(X) = J_2(X) + R_2(X) \quad ,$$

where

$$J_2(X) = \left[\frac{g''(X)}{g'(X)} - \frac{f'(X)}{f(X)}\right] \frac{f(X)e^{ikg(X)}}{(ikg'(X))^2} \quad ,$$

$$R_2(X) = \int_{-\infty}^{X} \frac{d}{dx}\left[\frac{d}{dx}\left[\frac{f(x)}{ikg'(x)}\right]\frac{1}{ikg'(x)}\right] e^{ikg(x)} dx \quad .$$

If f(x) were completely independent of k, we could apply the Riemann-Lebesgue lemma to show that, for n=1,2,

$$R_n(X) = o(k^{-n}) \quad , \quad k \to \infty \quad .$$

In fact f(x) depends weakly on k, but f(x) approaches a limit independent of k as $k\to\infty$ with other variables fixed (ref. 2, p.585). Thus I(X) has the following asymptotic approximation:

$$I(X) \sim J_1(X) + J_2(X) \quad , \quad k \to \infty \quad .$$

$J_1(X)$ and $J_2(X)$ are the first and second terms in what is approximately an asymptotic expansion of $I(X)$ in inverse powers of k. When k is large enough, $J_1(X) \gg J_2(X)$, so that we can safely approximate

$$I(X) \approx J_1(X). \qquad (6)$$

The above arguments do not tell us how large k should be in any particular case for approximation (6) to be valid. However, it is plausible that $R_2(X) \ll J_2(X)$ when $J_2(X) \ll J_1(X)$. Thus we can estimate the relative error in approximation (6) by the following upper bound on $|J_2(X)/J_1(X)|$:

$$E_r(X) = \left[\frac{g''(X)}{|g'(X)|} + \frac{3}{2}\left[\frac{1}{g_1(X)} + \frac{1}{g_2(X)}\right]\right]\frac{1}{k|g'(X)|} .$$

(To obtain this expression, $|f'(X)/f(X)|$ has been replaced by $(3/2)[1/g_1(X) + 1/g_2(X)]$, which is expected to be an upper bound on $|f'(X)/f(X)|$ in all cases (ref. 2, p.598).) We can estimate the absolute error in approximation (6) by the following upper bound on $|J_2(X)|$:

$$E_a(X) = E_r(X)\,\frac{|f(X)|}{k|g'(X)|} .$$

Both $E_r(X)$ and $E_a(X)$ are infinite at $X=x_r$ and tend to zero as $X \to -\infty$. Moreover, a graphical examination of $E_r(x)$ and $E_a(x)$ suggests that they are monotonic in $(-\infty, x_r)$, for typical geometries, admittance values and frequencies.

We move on to consider configurations for which still $X<x_r$ but $x_r - X$ is small enough for $E_r(X)$ and/or $E_a(X)$ to be unacceptably large. For the moment we require that both the source and receiver are many wavelengths above the boundary. The following breakdown of the integral is used:

$$I(X) = I(\tau) + K , \qquad (7)$$

where K is the integral over a truncated interval $\gamma_T=[\tau, X]$,

$$K = k\int_{\tau}^{X} G_{\beta_1}(\underset{\sim}{s},\underset{\sim}{t}_1)G_{\beta_2}(\underset{\sim}{s},\underset{\sim}{t}_2)dx ,$$

which will be evaluated numerically. We will choose τ so that we can satisfactorily approximate

$$I(\tau) \approx J_1(\tau) . \qquad (8)$$

To reduce the expense in evaluating K numerically we want to choose τ as close to x_r as possible while still insisting that approximation (8) should satisfy certain relative and absolute error criteria. We can uniquely define two upper limits, τ_r and τ_a, for τ by

$$E_r(\tau_r) = 0{\cdot}2 ,$$

$$E_a(\tau_a) = \epsilon , \qquad (9)$$

where ϵ is an arbitrary positive constant. $\tau \leq \tau_r$ ensures that $J_2(\tau)$ is sufficiently small compared to $J_1(\tau)$ for $E_a(\tau)$ to be an accurate estimate of the absolute error in approximation (8). Therefore, if also $\tau \leq \tau_a$, then the absolute error in the approximation (8) is $\leq \epsilon$. Thus by taking τ to be the minimum of τ_r and τ_a we ensure that the error made in replacing $I(\tau)$ by $J_1(\tau)$ in equation (7) is $\leq \epsilon$.

We can now consider the more general configuration in which x_r may be anywhere in relation to X, but the source and receiver remain many wavelengths above the boundary. If X is less than x_r, one of the above calculation methods applies. If X is greater than x_r, reciprocity can be invoked (reflect the problem in the plane x=L/2, then swap the source and receiver) and then one of the above methods applied.

Finally we note why the source and the receiver have so far been kept at least one wavelength above the boundary. If $\underset{\sim}{t}_1$ (or $\underset{\sim}{t}_2$) is very close to γ the approximation (6), which involves neglecting the integral $R_1(X)$ in equation (5), breaks down. This is because, for x in a small range of γ around $\underset{\sim}{t}_1$ (or $\underset{\sim}{t}_2$), f(x) changes rapidly with x. Thus the derivative of f(x) in the integrand of $R_1(X)$ is very large.

To avoid the consequent inaccuracies which may occur when $\underset{\sim}{t}_1$ or $\underset{\sim}{t}_2$ is within one wavelength of γ, an additional criterion is used for the choice of τ. We require τ to be small enough so that the line $x \leq \tau$ in γ is always at least one wavelength from $\underset{\sim}{t}_1$ and $\underset{\sim}{t}_2$.

GRAZING INCIDENCE RESULTS

Monofrequency Excess Attenuation

We can use the method described above for estimating φ_A to examine propagation over flat ground through a homogeneous still atmosphere. The monofrequency excess attenuation over geometrical spreading due to the presence of the ground can be approximated by

$$A_1 = 20\log_{10}\left|\frac{e^{ikd}}{4\pi d\ \varphi_A}\right| \quad \text{dB} \ . \qquad (10)$$

Propagation from a source above rigid ground to a receiver above absorbing ground has been examined. To model this problem β_1 was set to zero and the dependence of β_2 on frequency was calculated by the Delany and Bazley semi-empirical formula (refs. 9,10), with an effective flow resistivity of $10^5 \text{kgs}^{-1}\text{m}^{-3}$. This value was chosen as being a low value for grassland (ref. 11). (It is found that using two or three times this flow resistivity value causes only a small reduction in the magnitude of the A_1 results, and no change in the trends was observed.) Six configurations of source and receiver heights (h_s and h_r) were examined. Specifically, heights of 5m, 1·5m, and 0·5m were used, with $h_s \geq h_r$ in all cases. For each h_s and h_r combination calculations were carried out at four distances: L=250m, 500m, 1km, and 2km.

We will examine the significance of the proportion of rigid ground between the source and receiver. We can define a useful variable, p_r, by

$$p_r = X/L \ .$$

When the impedance discontinuity is between the source and receiver ($0 \leq X \leq L$), p_r gives the proportion of rigid ground between the source and receiver.

A sample of the results examined is shown in Figures 3a and 3b. Plots like those shown were calculated for all the octave band centre frequencies between 100Hz and 5kHz. Notice that, as is of course expected intuitively, when $p_r \leq 0$ or $p_r \geq 1$ the modelled ground behaves as an acoustically homogeneous plan, absorbing or rigid,

respectively. We therefore now concentrate the investigation only on the range $0 \leq p_r \leq 1$.

Figure 4(a) illustrates a simple curve shape that occurs whenever both kh_s and kh_r are small enough. Half of the plots examined were of this type. We see that A_1 increases monotonically with p_r. The gradient of each curve is greatest at the ends of the range of interest, i.e. near $p_r=0$ and $p_r=1$. At low enough frequencies the curves straighten out.

Figure 4(b) illustrates the disintegration of the orderly patterns seen in Figure 4(a) that occurs when h_s, h_r, or the frequency is increased sufficiently. About a third of the plots examined showed this type of disorderly pattern.

Figure 4(c) illustrates a different pattern that sometimes occurs when the source is higher than the receiver, but neither are so high above the boundary that the disorderly pattern seen in Figure 4(b) occurs. In Figure 4(c), A_1 is less dependent on the location of the impedance discontinuity when $p_r \leq 0{\cdot}3$. Notice that the right half of this plot shows the features observed in Figure 4(a). About a sixth of the plots examined showed this pattern.

When the orderly patterns seen in Figure 4(a) and the right hand side of Figure 4(c) occur, there is usually a range of octave band centre frequencies around 1kHz at which some or all of the curves on a plot are separated, in most of the range $0 \leq p_r \leq 1$, by about 3dB. This approximate 3dB increase in A_1 per doubling of L when propagation is over an admittance discontinuity occurs only for a range of values of kL. The start of this inhomogeneous absorbing ground effect corresponds with the start of a 6dB separation of the A_1 curves at $p_r \leq 0$, which occurs when $kL \approx 2300$. This 6dB increase in A_1 per doubling of L is a homogeneous absorbing ground effect which has been predicted theoretically (ref. 12). Figure 5 illustrates these observations. The range of plots examined show that the inhomogeneous ground effect fails to occur when kh_s or kh_r is large. This failure is observed in the left hand side of Figure 4(c).

Jet Engine Noise

We move on to examine the excess attenuation of a notional broad band environmental noise source. A simple spectral shape representative of a jet engine at full thrust is chosen. The free field 1m third octave band sound pressure level is taken as constant up to 200Hz, above which frequency it is reduced by 0·8dB per third octave band. Third octave band excess attenuations due to the presence of the ground are approximated here by A_1 values given by equation (10), using the band centre frequencies. To make the calculation more realistic we include the B.S.5727 (1979) third octave band free field air attenuations for 20°C and 70% relative humidity.

We consider only source and receiver heights of 1·5m so that the simple A_1 pattern illustrated in Figure 4(a) dominates the results. The process of intensity addition over the third octave bands will produce more moderate excess attenuations for the broad band noise than those calculated for monofrequency sound.

The excess attenuation of the broad band source noise caused by the presence of the ground and by air absorption along the propagation path is

$$A_2 = S_1 - (S_2 + 20\log_{10}L) \quad dB(A) \ ,$$

where S_1 is the total A-weighted sound pressure level of the notional source at 1m distance in the free field, and S_2 is the total A-weighted sound pressure level that we calculate at the receiver position.

Figure 6 shows how A_2 depends on p_r and L. We can see that it is not possible to predict the A_2 values at intermediate p_r from a linear interpolation between the values at p_r=0 and p_r=1. Notice however that, in the range $0{\cdot}25 \leqslant p_r \leqslant 0{\cdot}75$, A_2 appears to vary linearly with p_r. Also, in this range, A_2 increases by 5dB(A) per doubling of L. This dependence on L is in reasonable agreement with a commonly used 4dB(A) extra attenuation (of perceived noise level) per doubling of receiver distance from an aircraft source very close to the ground (of unspecified admittance) (ref. 13).

At L=1km and 2km, A_2 varies linearly with p_r in the range $0 \leqslant p_r \leqslant 0{\cdot}75$. This is useful because it means that $A_2(p_r)$ can be estimated from $A_2(0)$, the value for homogeneous absorbing ground, which is easier to calculate. The simple predictive equation, which is shown in Figure 5 for L=1km and 2km, is

$$A_2(p_r) = A_2(0) - 14{\cdot}7p_r \quad \text{dB(A)} \ , \quad 0 \leqslant p_r \leqslant 0{\cdot}75, \qquad (11)$$

Unfortunately we know of no practical results with which to compare this equation.

CONCLUSIONS

An improved calculation method has been presented for sound propagation over a straight line impedance discontinuity in flat ground. The method is restricted to the case when the impedance discontinuity is perpendicular to the direct source to receiver propagation path. The method is derived from an asymptotic analysis at large wavenumber of an approximate solution of a two dimensional boundary integral equation. Accuracy is adequate for the purpose of examining environmental noise propagation in ideal conditions. A limitation of the method is the assumption of homogeneous still air and flat ground.

Results for long distance grazing incidence monofrequency propagation show that the dimensionless heights (height multiplied by wavenumber) of the source and receiver above the ground are as important as the location of the impedance discontinuity. When these dimensionless heights are small enough, the results are very orderly, as illustrated by Figures 4(a) and (c).

Theoretical results for the excess attenuation, including air absorption, of a broad-band A-weighted notional environmental noise source have been examined. A few simple trends have been noted, in particular, equation (11).

REFERENCES

1. Thomasson, S.-I.: Reflection of Waves From a Point Source by an Impedance Boundary. J. Acoust. Soc. Amer., vol. 59, 1976, pp. 780-785.

2. Chandler-Wilde, S. N.: Ground Effects in Environmental Sound Propagation. Ph.D. Thesis, Bradford Univ., England, Dec. 1988.

3. Habault, D.: Sound Propagation Above an Inhomogeneous Plane: Boundary Integral Equation Methods. J. Sound Vib., vol. 100, 1985, pp. 55-67.

4. Chandler-Wilde, S. N.; Hothersall, D. C.: Integral Equations in Traffic Noise Simulation. In Computers in Mathematical Research (N.M. Stephens and M.P. Thorne, editors), Oxford University Press, 1988, pp. 207-235.

5. Chandler-Wilde, S. N.; Hothersall, D. C.: On the Green Function for Two-Dimensional Acoustic Propagation Above a Homogeneous Impedance Plane. Research Rep., Coventry Polytech., England, 1989.

6. Chandler-Wilde, S. N.; Hothersall, D. C.: Sound Propagation Above an Inhomogeneous Impedance Plane. J. Sound Vib., vol. 98, 1985, pp. 475-491.

7. Durnin, J.; Bertoni, H. L.: Acoustic Propagation Over Ground Having Inhomogeneous Surface Impedance. J. Acoust. Soc. Amer., vol. 70, 1981, pp. 852-859.

8. Klein, C.; Myncke, H.: Sound Field Above an Impedance Discontinuity. Proc. 3rd F.A.S.E. Congress, Göttingen, West Germany, Sept. 1982, pp. 471-474.

9. Delany, M. E.; Bazley, E. N.: Acoustical Properties of Fibrous Absorbent Materials. Applied Acoust., vol. 3, 1970, pp. 105-116.

10. Chessell, C. I.: Propagation of Noise Along a Finite Impedance Boundary. J. Acoust. Soc. Amer., vol. 62, 1977, pp. 825-34.

11. Embleton, T. F. W.; Piercey, J. E.; Daigle, G. A.: Effective Flow Resistivity of Ground Surfaces Determined by Acoustical Measurements. J. Acoust. Soc. Amer., vol. 74, 1983, pp. 1239-44.

12. Attenborough, K.: Review of Ground Effects on Outdoor Sound Propagation From Continuous Broadband Sources. Applied Acoust., vol. 24, 1988, pp. 289-319.

13. Davies, L. I. C.: A Guide to the Calculation of NNI. Direct. Operat. Res. Anal. Comm. 7908, 2nd Ed., C.A.A., London, 1981.

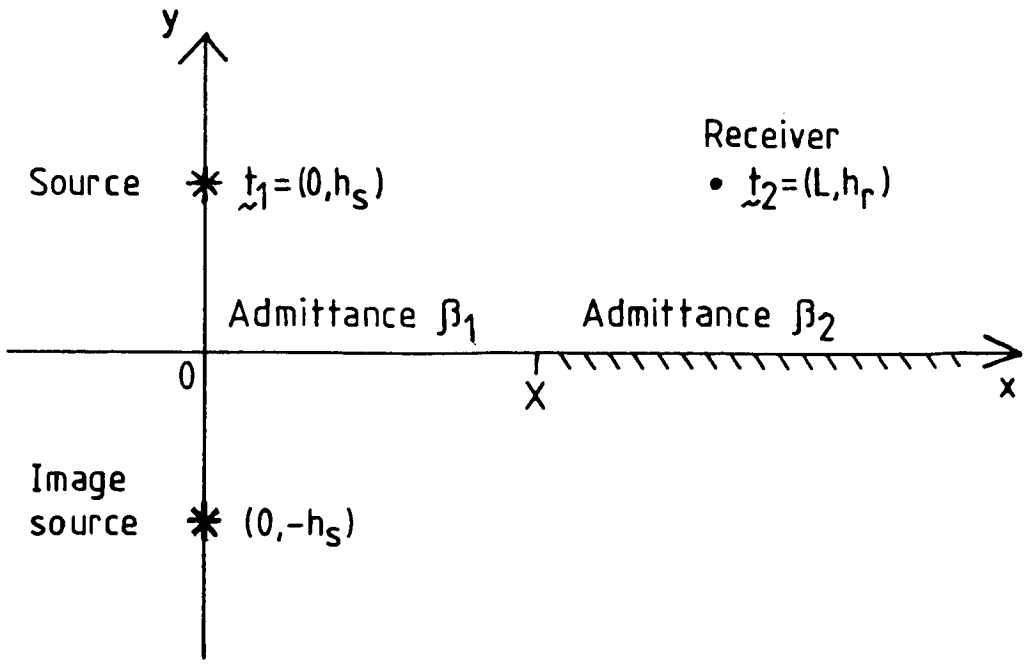

Fig.1 The problem in three dimensions.

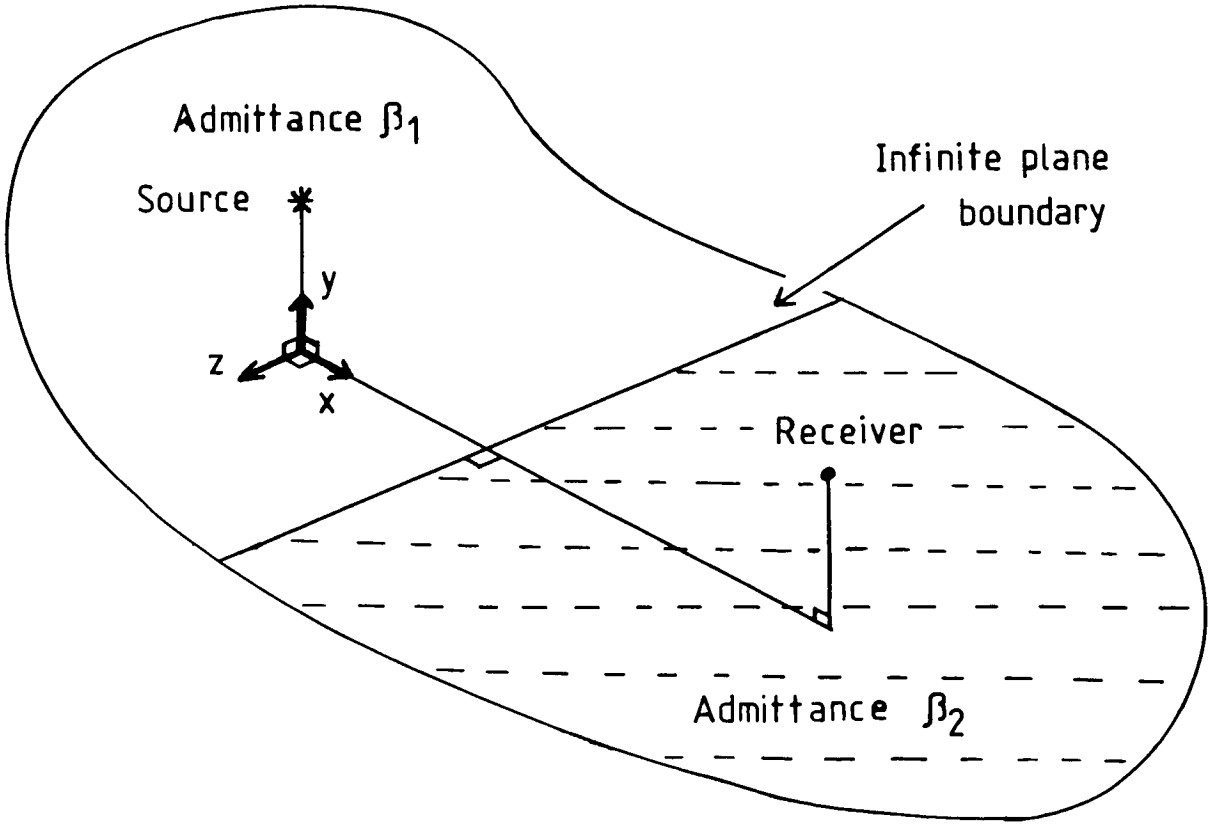

Fig.2 The problem in two dimensions.

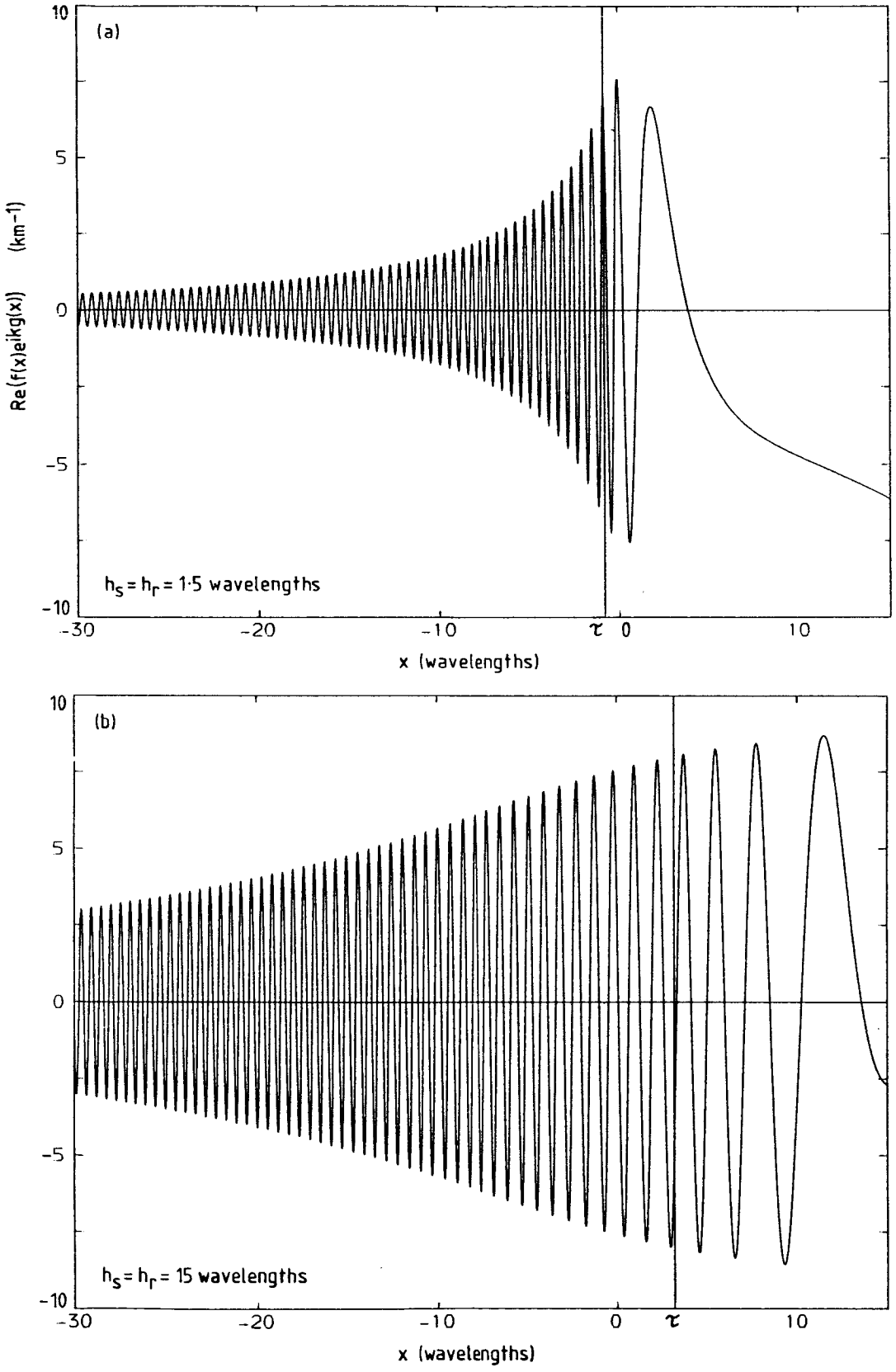

Fig.3 The real part of the integrand in the integral I(X), plotted against x over the range $1 \leq x \leq x_r$. L=30 wavelengths, β_1=0, β_2=0·13603-i0·13456.

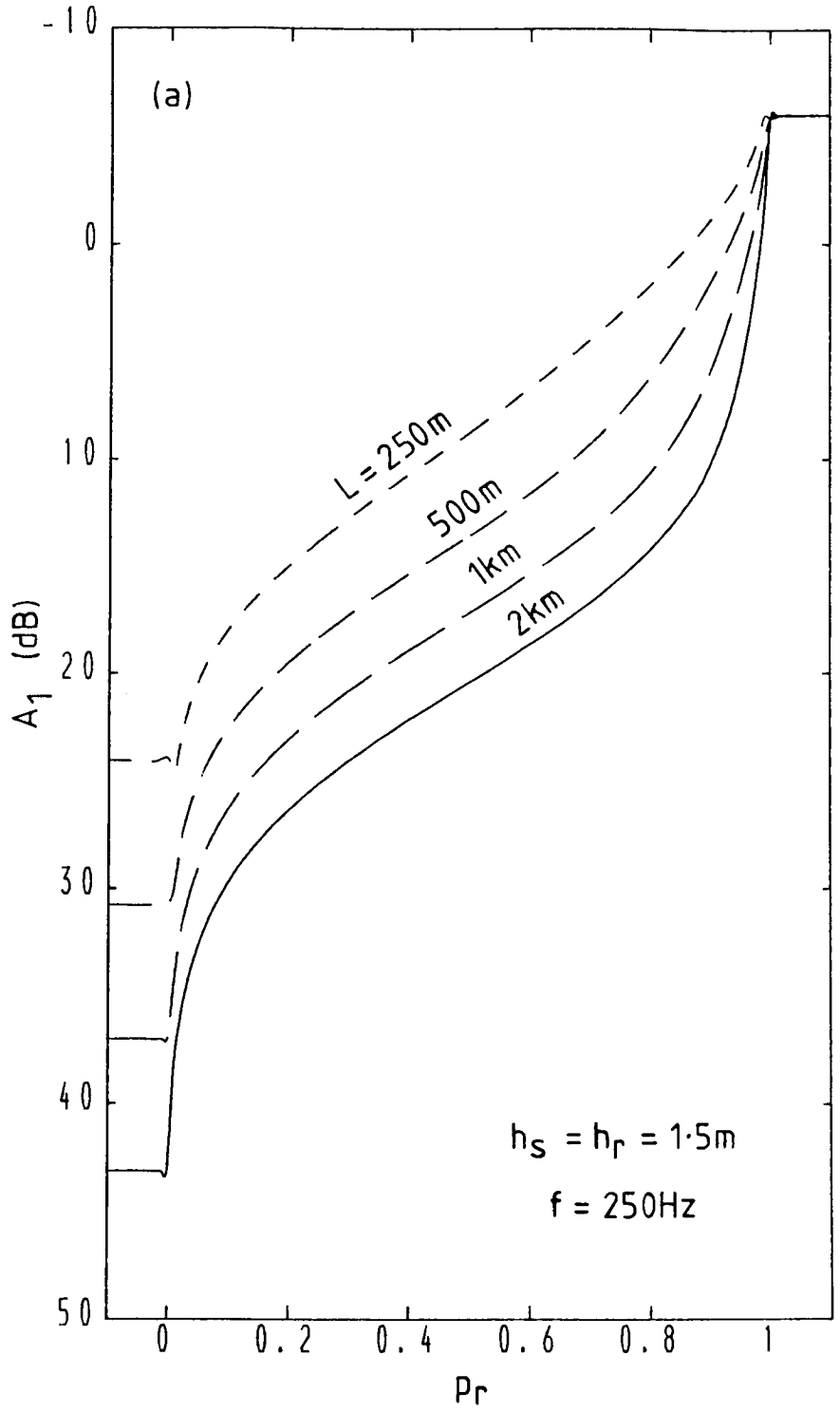

Fig.4a Monofrequency excess attenuation over geometrical spreading at four long distances, plotted against the proportion of rigid ground. h_s=h_r=1·5m, f=250Hz.

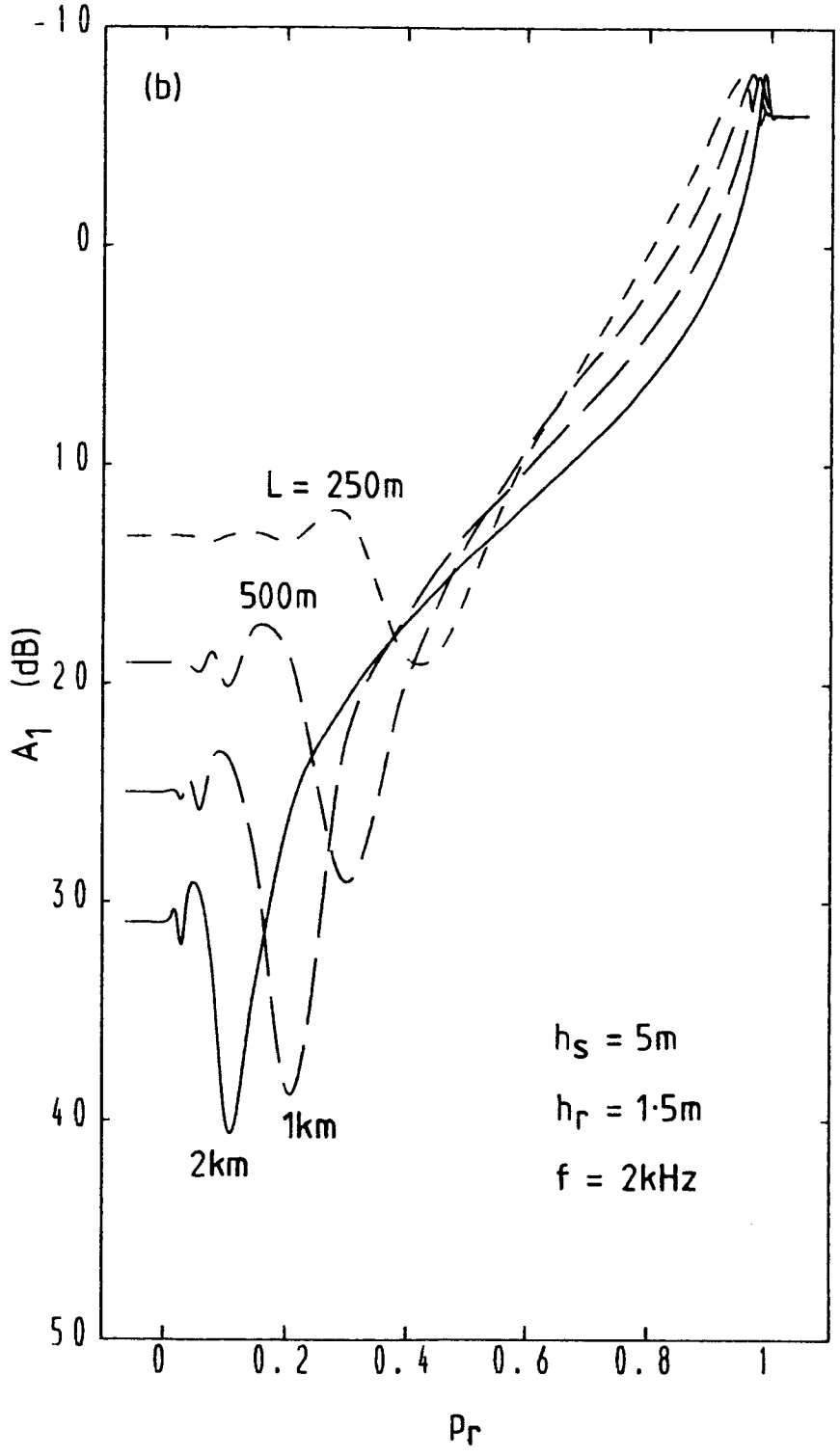

Fig.4b Monofrequency excess attenuation over geometrical spreading at four long distances, plotted against the proportion of rigid ground. h_s=5m, h_r=1.5m, f=2kHz.

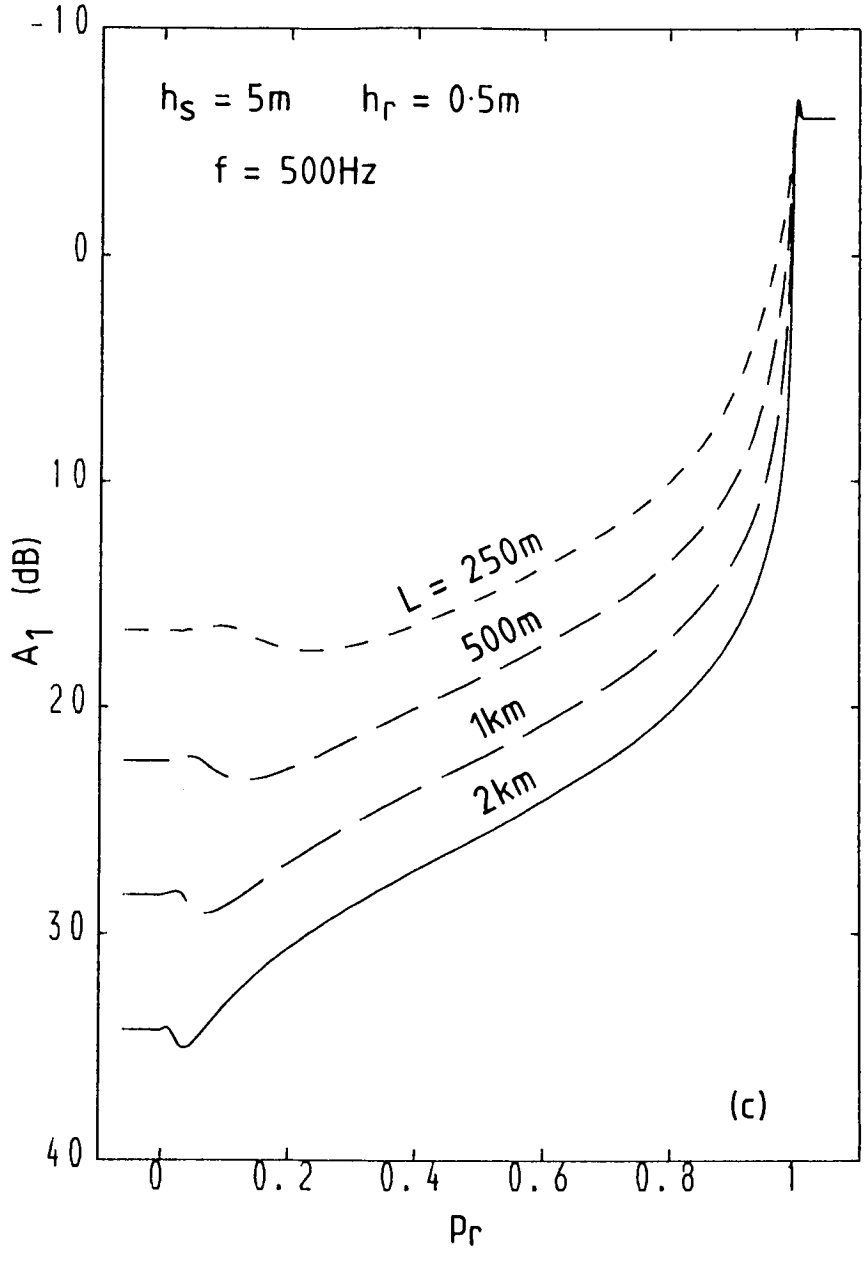

Fig.4c Monofrequency excess attenuation over geometrical spreading at four long distances, plotted against the proportion of rigid ground. h_s=5m, h_r=0.5m, f=500Hz.

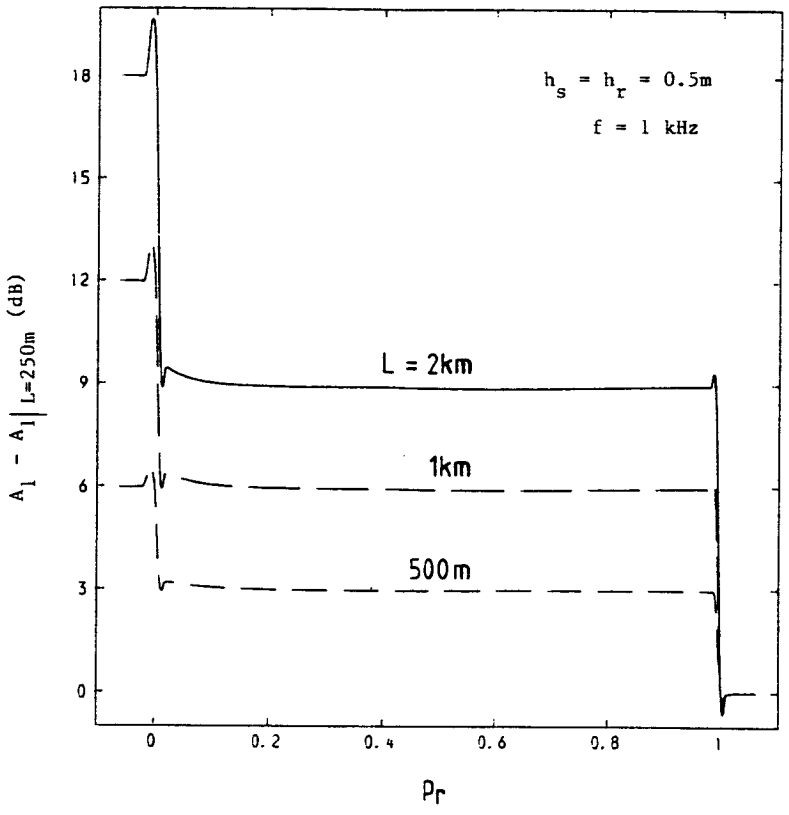

Fig.5 A_1 at L=500,1000,2000m relative to A_1 at L=250m, plotted against p_r.

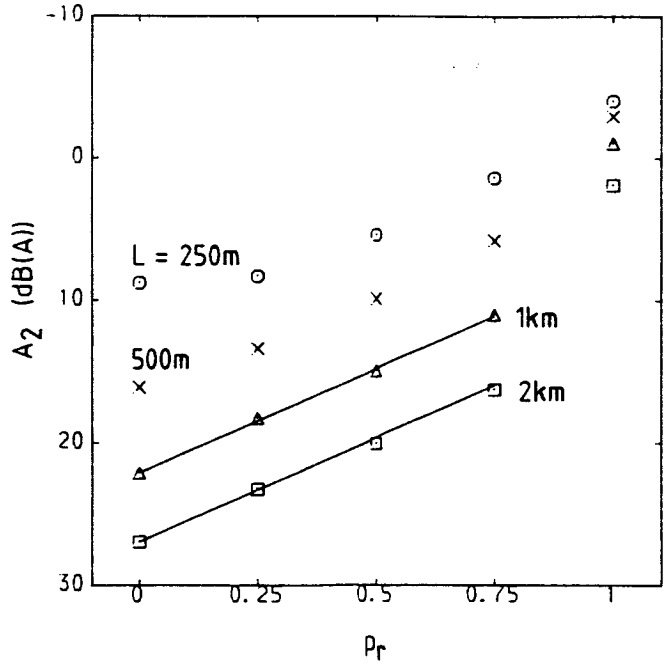

Fig.6 The attenuation of propagated noise from a notional jet engine source, plotted against p_r. Solid lines are equation (11).